Viscosity of Moderately Concentrated Isotropic Solutions of Xanthan, a Rigid Polyelectrolyte (Commemoration Issue Dedicated to Professor Hiroshi Ibagaki, Professor Michio Kurata, Professor Ryozo Kitamura, On the Occasion of Their Retirments)

AUTHOR(S):

Takada, Yasushi; Sato, Takahiro; Einaga, Yoshiyuki; Teramoto, Akio

Bull. Inst. Chem. Res., Kyoto Univ., Vol. 66, No. 3, 1988

Viscosity of Moderately Concentrated Isotropic Solutions of Xanthan, a Rigid Polyelectrolyte

Yasushi TAKADA, Takahiro SATO*, Yoshiyuki EINAGA**, and Akio TERAMOTO

Received September 29, 1988

Zero-shear-rate viscosity η_0 was measured for moderately concentrated isotropic solutions of xanthan as functions of polymer mass concentration c and added salt (NaCl) molar concentration C_s. η_0 steeply increased with increasing c, while it was essentially independent of C_s. Doi's expression for η_0 could fit to the c dependence by taking two constants in the expression as adjustable parameters. However, his theory failed to relate η_0 with the isotropic-liquid crystal phase boundary concentration depending strongly on C_s.

KEY WORDS: Zero-shear-rate Viscosity/ Xanthan/ Rigid polyelectrolyte/ Concentrated solution/ Doi's theory/

INTRODUCTION

A bacterial polysaccharide xanthan is a β-1, 4-D-glucan with an ionic trisaccharide side chain on the every two main chain glucose residues.[1] From dilute solution studies,[2-4] this polysaccharide was found to dissolve as a rigid double-stranded helix in aqueous salt solution. Thus xanthan is regarded as a rigid polyelectrolyte. The helix is stable at salt concentration $C_s \gtrsim 0.005$ M, if the solution temperature keeps at 25°C.[5]

Recently we[6] investigated the isotropic-cholesteric phase equilibrium in concentrated aqueous solution of xanthan and found that the phase boundary concentration strongly depends on C_s. This strong dependence exemplifies that the electrostatic interaction plays an important role in static properties of concentrated solutions of rigid polyelectrolyte, and stimulates us to study the role of the electrostatic interaction in dynamic properties of the same solutions. For this reason, we made zero-shear-rate viscosity measurements for the aqueous semi-dilute solutions of xanthan as functions of polymer mass concentration c and added salt (NaCl) molar concentration C_s. This paper describes the experimental results and compares them with Doi's theory for the semi-dilute solution viscosity of rodlike polymers.

EXPERIMENTAL

Sample Following the procedures established before,[3a] xanthan (Kelco's Keltrol) was sonicated, fractionated, and converted to the sodium salt form. The intrinsic viscosity

高田　育，寺本明夫：Department of Macromolecular Science, Osaka University Toyonaka, Osaka 560

* 佐藤尚弘：To whom correspondence should be addressed.

** 栄永義之：Present address: Department of Polymer Chemistry, Kyoto University, Kyoto 606

$[\eta]$ of the xanthan sample prepared was 5.77×10^2 cm^3/g at $C_s=0.1$ M and the viscosity-average molecular weight was estimated to be 5.9×10^5.[3b] A weighed amount of the sample was mixed with aqueous sodium chloride solution in a stoppered test tube and the mixture was stirred vigorously by a magnetic stirrer bar for more than 1 day.

Viscometry Viscosity measurements were made on a "floating-sphere rheometer" originally designed by Gordon et al.[7a] and improved by Pieranski et al.[7b] Fig. 1 shows a schematic diagram of this new rheometer. A steel sphere (B) with a radius a is made to float in a test solution by magnetic field gradient generated by a coil (C). To keep the sphere at a standstill the current through the coil is controled by the following servo-loop system. A halogen lamp (H) lights up the sphere, whose shadow, which is enlarged by a lens (L), is projected on two prisms. When the sphere moves, the shadowed portion on one of two prisms increases and that on the other one decreases. Then the photocurrents from two photodiodes (P_1, P_2) located behind the two prisms become different. This difference is fed into a PID amplifier, which controls the output current from a power amplifier. Finally, the current through the coil is changed so that the sphere (and its shadow) moves toward the equilibrium position where the photocurrent difference vanishes. The voltage U applied to the coil is monitored by a pen recorder.

When the test tube is moved downward (upward) at a constant velocity v by a step motor (M), the magnetic force $F_m(v)$ must increase (or decrease) according to

$$F_m(v)=F_m(0)\pm6\pi\eta av\psi \tag{1}$$

to keep the sphere at the equilibrium position. Here $F_m(0)$ is the magnetic force equilibrated at $v=0$, η the viscosity coefficient of the test solution, and ψ the correction

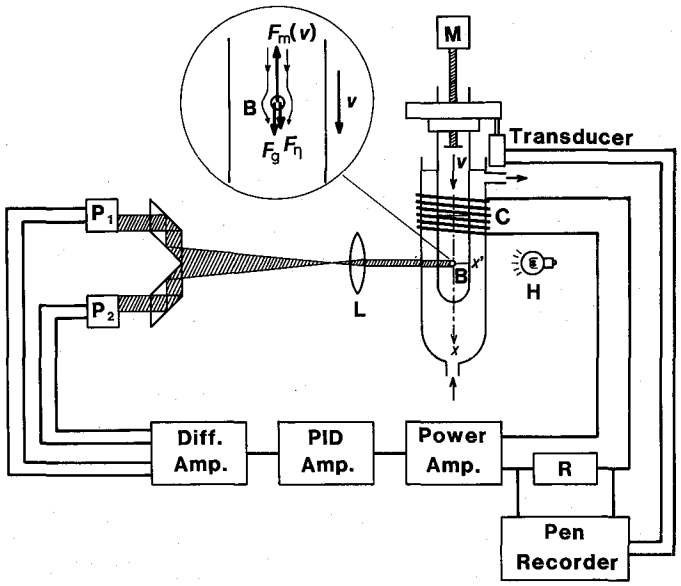

Fig. 1. Schematic diagram of "floating-sphere rheometer." (B) steel sphere; (C) coil; (H) halogen lamp; (L) lens; (P_1, P_2)Photodiodes; (M) step motor.

factor for the effect of tube wall.[8] $F_m(v)-F_m(0)$ should be proportional to the difference ΔU in U between at a finite v and zero, if ΔU is sufficiently small. Then η can be calculated from

$$\eta=[F_m(v)-F_m(0)]/6\pi av\psi$$
$$=(A/6\pi a)\Delta U/v \qquad (2)$$

where A is a proportionality constant and ΔU can be read from the pen recorder. The constant A was determined by use of silicone oil (η=9.6 P) and 95wt% aqueous glycerin (η=3.66 P). Fig. 2 shows the plots of $[F_m(v)-F_m(0)]/\psi$ against ΔU for the two test liquids, where $[F_m(v)-F_m(0)]/\psi$ was calculated from eq 1. At $\Delta U<50$ mV, data points for each sphere follow a straight line, whose slope gives A.

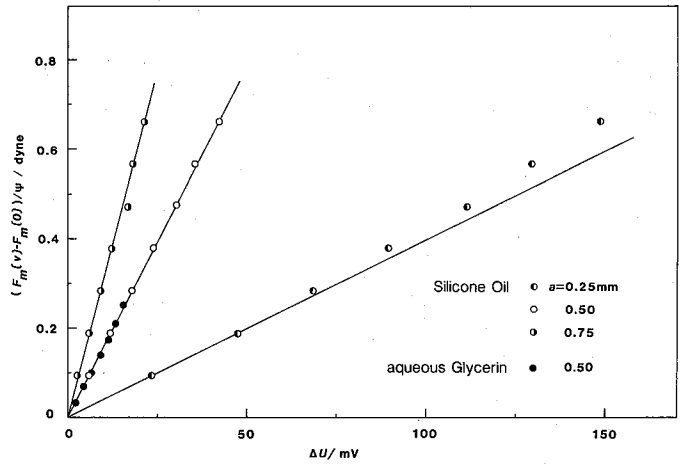

Fig. 2. Plots of $[F_m(v)-F_m(0)]/\psi$ vs. ΔU. The ordinate values were calculated from the values of η, a, and v by the equation $[F_m(v)-F_m(0)]/\psi=6\pi\eta av$.

Actual experiments were made using the sphere with a=0.5 mm and under the condition of $\Delta U<50$ mV. The inner diameter of the test tube used was 10 mm, while the sphere was kept at the center of the tube and more than 1 cm away from both the tube bottom and solution meniscus. The temperature of the solution was regulated by flowing water from a thermostat. For aqueous solutions, steel spheres coated with polystyrene were used.

In our experimental set up the flow field around the sphere was not uniform. Therefore the shear rate dependence of η was examined using the maximum shear rate $\dot{\gamma}$ at the equator of the sphere:

$$\dot{\gamma}=2a/3v$$

This floating-sphere rheometer can be used for viscosities up to about 10^5 P.

RESULTS

Fig. 3 shows the shear rate $\dot{\gamma}$ dependence of η for different c and C_s. In all cases, η is independent of $\dot{\gamma}$ in the range of $\dot{\gamma}$ examined and the zero-shear-rate viscosity η_0 can be determined without difficulty. The values of η_0 obtained are listed in Table 1. In Fig. 4, η_0 are double-logarithmically plotted against c. Different symbols represent the data for different C_s and the arrow indicates the phase boundary concentration c_i between the isotropic and biphasic regions for each C_s, which was determined by the usual method.[9] It can be seen that η_0 steeply increases with c and does not obey a simple power law of c. The exponent at $c=c_i$ ranges from 3.4 to 6.5 depending on C_s; the value of η_0 at c_i also strongly depends on C_s (see Table 2).

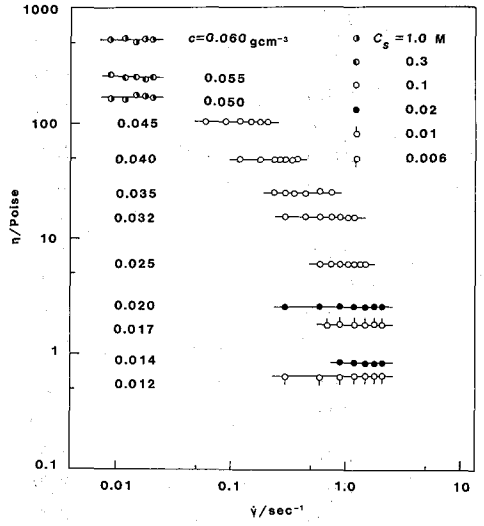

Fig. 3. Shear rate dependence of viscosity for aqueous xanthan with different c and C_s.

It is important to note in Fig. 4 that η_0 is almost independent of C_s. In a previous dilute solution study,[10] the intrinsic viscosity $[\eta]$ of sodium salt xanthan in aqueous salt was found to be almost independent of C_s. This means that the chain dimension of xanthan is essentially constant irrespective of the strength of the intramolecular electrostatic repulsion and is explained by the large non-electrostatic persistence length ($\sim$110 nm) of xanthan compared with the electrostatic one. Thus the insensitivity of η_0 to C_s shown in Fig. 4 implies that the intermolecular electrostatic interaction which varies remarkably with C_s does not affect the viscosity of the semi-dilute solutions.

Table 1. The values of the zero-shear viscosity η_0 for aqueous xanthan as functions of C_s and c.

C_s/M	$c/10^{-2}$ gcm^{-3}	η_0/P
0.006	0.100	0.016
	0.133	0.019
	0.200	0.026
	0.250	0.033
	0.333	0.048
	0.400	0.063
	0.801	0.237
	1.00	0.410
	1.20	0.651
	1.30	0.833
	1.41	1.07
	1.50	1.35
0.010	0.100	0.015
	0.200	0.026
	0.400	0.060
	0.500	0.088
	0.800	0.218
	1.00	0.372
	1.20	0.598
	1.40	0.985
	1.50	1.19
	1.70	1.81
	1.80	2.48
0.020	0.100	0.016
	0.200	0.025
	0.500	0.084
	0.700	0.154
	1.00	0.348
	1.20	0.555
	1.40	0.840
	1.50	0.997
	1.70	1.55
	1.80	1.83
	2.00	2.60
	2.20	4.14
0.100	0.500	0.081
	1.00	0.337
	1.50	0.981
	1.80	1.82
	2.00	2.57
	2.50	5.97
	3.00	11.4
	3.20	15.5
	3.50	25.0
	3.80	44.4
	4.00	49.4
	4.50	104
0.300	1.00	0.327
	2.00	2.44
	3.00	11.4
	4.00	42.7
	5.00	140
	5.50	253
	6.00	291
1.00	0.100	0.018
	0.500	0.092
	1.00	0.381
	2.00	2.90
	3.00	14.7
	3.80	39.8
	4.50	95.0
	5.00	170
	5.50	291
	6.00	530
	6.20	622
	6.50	851
	6.80	1137
	7.00	1626
	7.10	1657
	7.20	1890
	7.40	2030

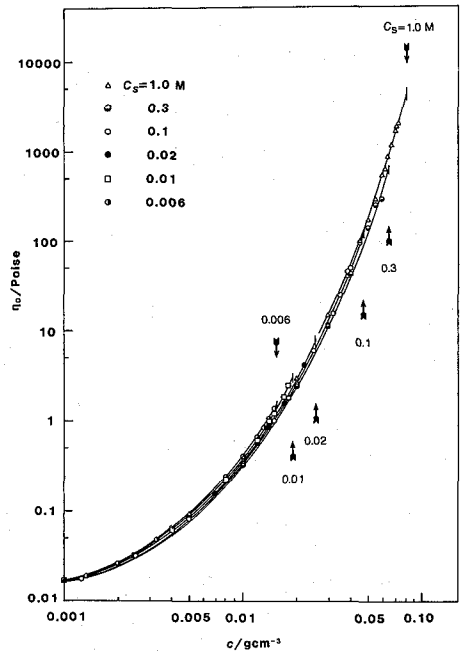

Fig. 4. Double-logalithmic plots of η_0 vs. c for different C_s. The arrows in the figure indicate the isotropic-liquid crystal phase boundary concentration c_i.

Table 2. The Values of η_0 and the exponent ε at the phase boundary concentration c_i for aquous xanthan with different C_s.

C_s/M	c_i/gcm^{-3}	$\eta_0(c_i)$/P	$\varepsilon(c_i)$*
0.006	0.0155	1.55	3.4
0.01	0.0191	3.02	3.9
0.02	0.0252	7.94	4.2
0.10	0.0475	135	5.6
0.30	0.065	724	6.2
1.00	0.080	3310	6.5

*$\eta_0 \propto c^{\varepsilon(c)}$

DISCUSSION

The zero-shear viscosity η_0 of a moderately concentrated isotropic solution of a rodlike polymer can be related to the rotational diffusion coefficient D_r of the rod at same concentration by the equation[11)]

$$\eta_0 = RTc/10MD_r \tag{3}$$

where R is the gas constant, T the absolute temperature, and M the polymer molecular weight. The rigorous calculation of D_r for a rod interacting with surrounding rods is very difficult but Doi[12)] derived an approximate expression of D_r using the following

model: the rotational Brownian motion of a "test rod" is restricted for a moment by the entanglement interaction with surrounding rods. However when this restriction is removed by the translational motion of the surrounding rod, the test rod can rotate by a small angle $l/(L/2)$, where L is the length of rod and l is the step length on the spherical surface with the radius $L/2$. After this process is repeated many times, the rotational diffusion of the test rod occurs. Assuming the translational diffusion coefficient D_t of the test rod in semi-dilute solution to be equal to that at infinite dilution, Doi obtained the expression

$$D_r = k^{-1} D_{ro} / (M^4 c^2 N_A^2 / M_L^6) \tag{4}$$

Here D_{ro} is D_r at infinite dilution, N_A the Avogadro number, M_L the molecular weight per unit length of the rod, and k a constant. From eq 3 and 4, η_0 can be written as

$$\eta_0 = k(RT/10D_{ro})(cM)^3 N_A^2 / M_L^6 \tag{5}$$

Doi and Edwards[13] derived the same expression using a tube model.

Equation 5 predicts that η_0 should be proportional to c^3. However, many experimental results[14-16] including the data shown in Fig. 4 and Table 2 reveal that this concentration dependence holds only in a very narrow range of concentration. Near the phase boundary concentration c_t, the dependence is much stronger than c^3. To explain this strong concentration dependence, Doi[12] replaced the step length l by $l-d$ (d: diameter of the rod) and obtained

$$\eta_0 = k(RT/10D_{ro})[(cM)^3 N_A^2 / M_L^6][1-(N_A d/\alpha)(cM/M_L^2)]^{-2} \tag{6}$$

with another constant α. From the viewpoint of the tube model, the reduction of l was interpreted as the fact that the tilting angle of the test rod escaping from the tube is diminished by the finite thickness of the rod.[17]

In general, D_{ro} is related to the intrinsic viscosity $[\eta]$ by[18]

$$D_{ro} = 2RT/15\eta_s M[\eta] \tag{7}$$

where η_s is the solvent viscosity. Combination of eq 6 with eq 7 gives[14,15]

$$\eta_0/\eta_s M[\eta] = K(cM)^3/[1-\beta(cM)]^2 \tag{8}$$

where $K = 3kN_A^2/4M_L^6$ and $\beta = N_A d/\alpha M_L^2$. In this theory β is used as a measure for the repulsive interaction between rods. However it is not clear whether it is a thermodynamic parameter or a hydrodynamic one.

Fig. 5 displays the plot of $([\eta]M^4c^3/\eta_0)^{1/2}$ vs. cM for aqueous xanthan with different salt concentrations. Here, only the data for $c \geq 0.01$ gcm^{-3} are plotted. The concentration 0.01 gcm^{-3} is about ten times higher than the overlap concentration c^* which is calculated to be 7×10^{-4} gcm^{-3} from the relation $c^* = 3M/4\pi\langle S^2\rangle^{3/2}N_A$ ($\langle S^2\rangle^{1/2}$: radius of gyration of the polymer) using the $\langle S^2\rangle^{1/2}$-M relation obtained before.[3b] Except at low c and near the phase boundary concentration, the data points for all C_s

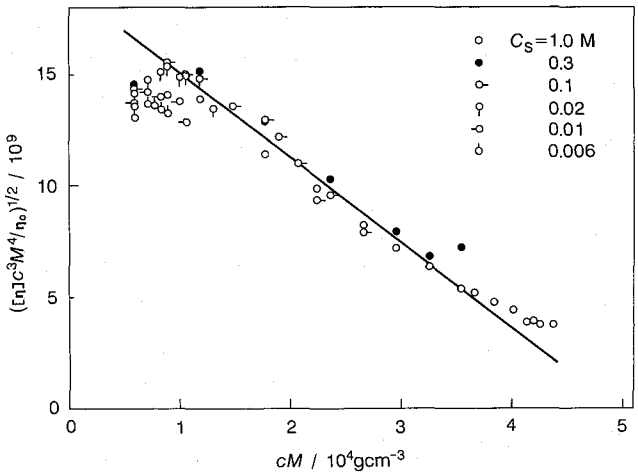

Fig. 5. Plots of $([\eta]M^4c^3/\eta_0)^{1/2}$ vs. cM for aqueous xanthan with different C_s. The ordinate has the units of $(g^5s/cm^5mol^4)^{1/2}$.

almost follow a single straight line.† Thus the functional form of eq 8 is suitable for representing the concentration dependence of η_0 of aqueous xanthan. The straight line in Fig. 5 gives $K=3.1\times10^{-19}$ cm^{6}mol^{4}g^{-6} and $\beta=2.0\times10^{-5}$ cm^{3}molg^{-2}. From these K and β values along with $M_L=1940$ nm^{-1} and $d=2.2$ nm, k and α are estimated to be 6.2×10^{-5} and 17.4, respectively. So far, successful fittings of η_0 to eq 8 have been demonstrated for several stiff polymer solutions, for example, aqueous schizophyllan[14] and poly(p-phenylene-2, 6-benzobisthiazole) (PBT) in methanesulfonic acid (MSA).[15] The reported values of α are 8.8 (aqueous schizophyllan) and 16.2 (PBT in MSA): α for aqueous xanthan is closer to the latter value. The k value for rodlike schizophyllan is 5.6 x 10^{-4}, which is much larger than k for xanthan. Our xanthan sample used in this study is not a completely rigid rod. Therefore the small k for aqueous xanthan may be attributed to the flexibitity of the xanthan molecule.

Equation 8 is often rewritten[12,14,15] as

$$\eta_0/\eta_s M[\eta]=K(cM)^3/[1-B(c/c_{cr})]^2 \qquad (8')$$

using a critical concentration c_{cr} and a constant B; c_{cr} approximately equals c_i. Since the experimental data for η_0 of aqueous xanthan is almost independent of C_s, c_{cr} should be approximately constant. But, actually, it is experimentally[6] shown that c_i for aqueous xanthan strongly depends on C_s. Thus eq 8' fails to relate η_0 with the phase boundary concentration for aqueous xanthan. Originally Doi's theory was proposed for rods interacting only with the hard-core potential. However eq 8' has been derived by identifying d in eq 6 with the thermodynamic effective diameter[19] which can be related to the phase boundary concentration for polyelectrolyte solutions. Thus this

† With lowering c, the viscosity related to the hydrodynamic energy dissipation becomes important,[11] which is neglected in eq 3. Thus the downward deviation of the data points from the straight line at low c can be mainly due to the neglect of this viscosity term. (Another cause may be the inapplicability of Doi's rotational diffusion mechanism at low concentration.)

identification is considered to cause the inconsistency of eq 8' with the experiment which suggests that d in eq 6 has to be regarded as the hard-core diameter of the polyelectrolyte. There is no theoretical justification for this suggestion, which invites a further theoretical study of the problem.

ACKNOWLEDGMENT

This work was finantially supported by a Grant-in-Aid for Scientific Research, 61470102, from the Ministry of Education, Science, and Culture of Japan.

REFERENCES

(1) P. E. Jannson, L. Kenne, and B. Lindburg, *Carbohydr. Res.*, **45**, 275 (1975).
(2) G. Paradossi and D. A. Brant, *Macromolecules*, **15**, 874 (1982).
(3) (a) T. Sato, T. Norisuye, and H. Fujita, *Polym. J.*, **16**, 341 (1984); (b) T. Sato, S. Kojima, T. Norisuye, and H. Fujita, *Polym. J.*, **16**, 423 (1984); T. Sato, T. Norisuye, and H. Fujita, *Macromolecules*, **17**, 2696 (1984).
(4) T. Coviello, K. Kajiwara, W. Burchard, M. Dentini, and V. Crescenzi, *Macromolecules*, **19**, 2826 (1986).
(5) W. Liu, T. Sato, T. Norisuye, and H. Fujita, *Carbohydr. Res.*, **160**, 267 (1987).
(6) T. Sato, T. Kakihara, and A. Teramoto, Preprints, IUPAC 32nd International Symposium on Macromolecules, Kyoto, Japan, 1988, p. 395.
(7) (a) M. Gordon, S. C. Hunter, J. A. Love, and T. C. Ward, *Nature*, **217**, 735 (1968); (b) B. Gauthier-Manuel, R. Meyer, and P. Pieranski, *J. Phys. E: Sci. Instum.*, **17**, 1177 (1984); M. Adam, M. Delsanti, P. Pieranski, and R. Meyer, *Rev. Phys. Appl.*, **19**, 253 (1984).
(8) R. Landenburg, *Ann. Phys.*, **23**, 447 (1907).
(9) T. Itou and A. Teramoto, *Macromolecules*, **21**, 2225 (1988).
(10) T. Sho, T. Sato, and T. Norisuye, *Biophys. Chem.*, **25**, 307 (1986).
(11) M. Doi and S. F. Edwards, "The Theory of Polymer Dynamics," Oxford Univ. Press, London 1986.
(12) M. Doi, *J. Physique*, **36**, 607 (1975).
(13) M. Doi, and S. F. Edwards, *J. Chem. Soc. Faraday II*, **74**, 560, 918 (1978).
(14) H. Enomoto, Y. Einaga, and A. Teramoto, *Macromolecules*, **17**, 1573 (1984); **18**, 2695 (1985).
(15) S.-G. Chu, S. Venkatraman, G. C. Berry, and Y. Einaga, *Macromolecules*, **14**, 939 (1981).
(16) D. G. Baird and R. L. Ballman, *J. Rheol. (N.Y.)*, **23**, 505 (1979).
(17) M. Doi, *J. Polym. Sci.: Polym. Phys. Ed.*, **19**, 229 (1981).
(18) H. Yamakawa, "Modern Theory of Polymer Solutions," Harper & Low, New York (1971).
(19) L. Onsager, *Ann. N.Y. Acad. Sci.*, **51**, 627 (1949).